This is a repository copy of *Eco-Evolutionary Dynamics of a Population with Randomly Switching Carrying Capacity*.

White Rose Research Online URL for this paper:
http://eprints.whiterose.ac.uk/133883/

Version: Accepted Version

Eco-Evolutionary Dynamics of a Population with Randomly Switching Carrying Capacity

Karl Wienand,[1] Erwin Frey,[1] and Mauro Mobilia[2, *]

[1]*Arnold Sommerfeld Center for Theoretical Physics, Department of Physics,*
Ludwig-Maximilians-Universität München, Theresienstrasse 37, 80333 München, Germany
[2]*Department of Applied Mathematics, School of Mathematics, University of Leeds, Leeds LS2 9JT, U.K.*

Environmental variability greatly influences the eco-evolutionary dynamics of a population, i.e. it affects how its size and composition evolve. Here, we study a well-mixed population of finite and fluctuating size whose growth is limited by a randomly switching carrying capacity. This models the environmental fluctuations between states of resources abundance and scarcity. The population consists of two strains, one growing slightly faster than the other, competing under two scenarios: one in which competition is solely for resources, and one in which the slow ("cooperating") strain produces a public good that benefits also the fast ("freeriding") strain. We investigate how the coupling of demographic and environmental (external) noise affects the population's eco-evolutionary dynamics. By analytical and computational means, we study the correlations between the population size and its composition, and discuss the social-dilemma-like "eco-evolutionary game" characterizing the public good production. We determine in what conditions it is best to produce a public good; when cooperating is beneficial but outcompeted by freeriding, and when the public good production is detrimental for cooperators. Within a linear noise approximation to populations of varying size, we also accurately analyze the coupled effects of demographic and environmental noise on the size distribution.

Keywords: population dynamics, evolution, ecology, fluctuations, cooperation dilemma, public goods

I. INTRODUCTION

The fate of populations is affected by a number of endlessly changing environmental conditions such as the presence of toxins, resources abundance, temperature, light, etc. [1, 2]. In the absence of detailed knowledge of how external factors vary, they are modeled as external noise (EN) shaping the randomly changing environment in which species evolve. The impact of fluctuating environments on population dynamics has been studied in a number of systems [3–14], and several evolutionary responses to exogenous changes have been analyzed [15–21]. In finite populations, internal noise is another important form of randomness, yielding demographic fluctuations of stronger intensity in small populations than in large ones. Internal noise (IN) is responsible for fixation [22–24] (when one species takes over and others are wiped out) and thus plays an important role in the evolution of a population's composition. Ecological and evolutionary dynamics are often coupled, through an interdependent evolution of the population size and composition [25–31]. As a consequence, environmental variability may affect the population size and hence the demographic fluctuations intensity, thus coupling EN and IN. The interdependence of environmental noise and demographic fluctuations is particularly relevant for microbial communities, whose properties greatly depend on the population size and on the environment [1, 2]. These populations often experience sudden environmental changes that can drastically affect their size, *e.g.* by leading to *population bottlenecks* under which the colony of reduced size is more prone to fluctuations [32–35]. The coupling between the different forms of randomness therefore generates feedback loops between socio-biological interactions and the environment [32, 33, 36, 37], which results in fascinating eco-evolutionary phenomena such as cooperative behavior. For instance, experiments on *Pseudomonas fluorescens* showed that the formation and sudden collapse of biofilms promotes the evolution of cooperation [34, 35, 38]. In most studies, however, EN and IN are treated as uncoupled [4–14].

Recently, we introduced a model describing a fluctuating population—consisting of a fast strain competing with a slow (cooperating) species, that can produce a public good—evolving under a randomly switching carrying capacity [39]. In this model, *demographic fluctuations are coupled to EN*, resulting in a significant influence on the species fixation probability and leading to noise-induced transitions of the population size. In the context of the eco-evolutionary dynamics of this model, here we introduce the theoretical concept of "eco-evolutionary game" to characterize the emergence of cooperation in populations of fluctuating size. We study the correlations between the population size and its composition and show that a social dilemma of sorts arises: while the public good production increases the overall expected population size, it also lowers the survival probability of cooperators. In the biologically-inspired setting of a metapopulation of non-interacting communities of varying size, we measure the success of each species in the eco-evolutionary game in terms of its expected long-term number of individuals. We thus determine the circumstances under which public good production (cooperation) is detrimental or beneficial to cooperators, and find the conditions in which it is best to produce the public good. Furthermore, we have devised a linear noise approximation that allows us to accurately characterize the population size distribution and noise-induced transitions in a population whose size fluctuates under the joint effect of coupled demographic and environmental noise.

The next two sections establish our approach: In section II, we introduce our stochastic model; in section III, we outline the properties of the fitness-dependent Moran model and piecewise deterministic Markov processes associated with the
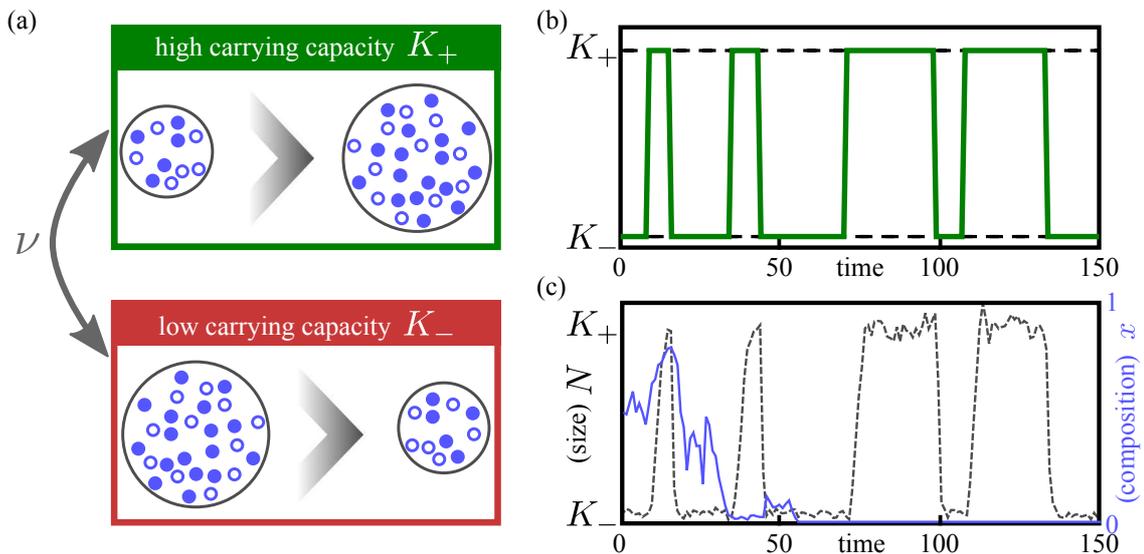
FIG. 1: (a) Cartoon of the eco-evolutionary dynamics of the model: the population consists of strains S ($\circ$) and F ($\bullet$), subject to $K(t) \in \{K_-, K_+\}$ that randomly switches, see (4). After each switch of $K(t)$, N and x change: following a K_- to K_+ switch, N increases and the intensity of the internal noise decreases; the opposite occurs following a K_+ to K_- switch. (b) Typical random switching of $K(t)$ according to (4). (c) Sample paths of $N(t)$ (gray, dashed line) and $x(t)$ (blue, solid line), corresponding to the switching portrayed in (b). We notice that x evolves much slower than N, see text. Parameters are $(s, \nu, K_+, K_-, b) = (0.02, 0.1, 450, 50, 0)$.

model, and review how to combine these to compute the species fixation probabilities. In the following two sections, we present our main results: Section IV is dedicated to the correlations between the population size and its composition, and to the discussion of the emergence of cooperative behavior along with an "eco-evolutionary game" in a population of fluctuation size; in section V, we study the population size distribution within a linear noise approximation. Our conclusions are presented in Sec. VI. Additional information is provided in the Supplementary Material (SM) [40].

II. MODEL

As in our recent work [39], we consider a well-mixed population of fluctuating size $N(t) = N_S(t) + N_F(t)$, consisting of N_S individuals of species S and N_F of species, or strain, F [42]. The fast-growing strain F has fitness $f_F = 1$, whereas the slow-growing strain S has a slightly lower fitness $f_S = 1 - s$, where $0 < s \ll 1$ denotes the (weak) selection intensity. At time t the fraction of S individuals in the population is $x(t) = N_S(t)/N(t)$ and the average population fitness is $\bar{f} = xf_S + (1 - x)f_F = 1 - sx = 1 + \mathcal{O}(1)$. Here, the evolution of the population size $N(t)$ is coupled to the internal composition $x(t)$ by a global growth rate $g(x)$, and its growth is limited by a logistic death rate $N/K(t)$ [25–27, 39]. The carrying capacity $K(t)$ is a measure of the population size that can be supported, and is here assumed to vary in time, see below. We specifically focus on two important forms of global growth rates: (i) the *pure resource competition* scenario $g(x) = 1$, in which x and N are coupled only through fluctuations; and (ii) the *public good scenario* in which $g(x) = 1 + bx$, corresponding to a situation where S

individuals are "cooperators" [25–27, 41] producing a public good (PG) that enhances the population growth rate through the benefit parameter $0 < b = \mathcal{O}(1)$, here assumed for simplicity to be independent of s. In the PG scenario, N and x are explicitly coupled, since the changes in the size of the population (*ecological dynamics*) and those in its composition (*evolutionary dynamics*) are interconnected. This interplay establishes a form of "eco-evolutionary dynamics" [28, 29]. It is worth noting that, as customary in evolutionary game theory, we assume that mutation rates of the strains are negligible, and we thus characterize the population evolutionary dynamics in terms of the fixation properties [24, 41].

In this context, the population size and composition change according to the continuous-time birth-death process [26, 45, 46]

$$N_{S/F} \xrightarrow{T^+_{S/F}} N_{S/F} + 1 \quad \text{and} \quad N_{S/F} \xrightarrow{T^-_{S/F}} N_{S/F} - 1, \quad (1)$$

with transition rates

$$T^+_{S/F} = g(x)\frac{f_{S/F}}{\bar{f}}N_{S/F} \quad \text{and} \quad T^-_{S/F} = \frac{N}{K(t)}N_{S/F}. \quad (2)$$

We model environmental randomness by letting the carrying capacity $K(t)$ switch randomly between K_+ (abundant resources) and $K_- < K_+$ (scarce resources), see figure 1(a,b). We assume that $K(t)$ switches at rate ν, according to a time-continuous symmetric dichotomous Markov noise (DMN) [43, 44, 47] $\xi(t) \in \{-1, +1\}$ (or *random telegraph noise*):

$$\xi \xrightarrow{\nu} -\xi, \quad (3)$$

The stationary symmetric DMN has zero-mean $\langle \xi(t) \rangle = 0$ and autocorrelation $\langle \xi(t)\xi(t') \rangle = \exp(-2\nu|t - t'|)$ ($\langle \cdot \rangle$ denotes the ensemble average over the environmental noise) [43,

44]. This is a *colored noise* with a finite correlation time $1/(2\nu)$ [43, 44, 47–50], see Section 1 in SM [40]. As a result, the fluctuating carrying capacity reads

$$K(t) = \frac{1}{2}\left[(K_+ + K_-) + \xi(t)(K_+ - K_-)\right], \qquad (4)$$

and endlessly switches between K_+ and K_-.

In what follows, we consider that the DMN is stationary: $\langle\xi(t)\rangle = 0$ for $t \geq 0$. Hence, the initial carrying capacity is either K_- or K_+ with probability $1/2$, and the average carrying capacity is constant: $\langle K(t)\rangle = \langle K\rangle = (K_+ + K_-)/2$.

The DMN models suddenly changing conditions, reflecting several situations in bacterial life, such as cells living at either side of a physical phase transition [1], or in the ever-changing conditions of a host digestive tract. In the laboratory, bacteria can be subjected to complex gut-like environment [54] or simplified stressful conditions, typically through variable exposure to antibiotics [55–57]. Furthermore, with modern bioengineering techniques it is possible to perform controled microbial experiments in settings allowing for sensible comparisons with theoretical models sharing some of the features considered here (switching environment, time-varying population size, public good production) [16, 17, 30, 36]. As discussed in Section IV.B, the setting where colonies of bacteria are grown in arrays of wells or test tubes [30, 36], modeled as a metapopulation of communities, is particularly relevant for our purposes.

In this model, the population evolves according to the multivariate stochastic process defined by equation (1)-(4), which obeys the master equation

$$\begin{aligned}
\frac{dP(\vec{N},\xi,t)}{dt} &= (\mathbb{E}_S^- - 1)[T_S^+ P(\vec{N},\xi,t)] \\
&+ (\mathbb{E}_F^- - 1)[T_F^+ P(\vec{N},\xi,t)] \\
&+ (\mathbb{E}_S^+ - 1)[T_S^- P(\vec{N},\xi,t)]] \\
&+ (\mathbb{E}_F^+ - 1)[T_F^- P(\vec{N},\xi,t)] \\
&+ \nu[P(\vec{N},-\xi,t) - P(\vec{N},\xi,t)], \qquad (5)
\end{aligned}$$

where $\vec{N} = (N_S, N_F)$, $\mathbb{E}_{S/F}^\pm$ are shift operators such that $\mathbb{E}_S^\pm G(N_S, N_F, \xi, t) = G(N_S \pm 1, N_F, \xi, t)$ for any $G(N_S, N_F, \xi, t)$, and similarly for $\mathbb{E}_F^\pm$.

Equation (5) fully describes the stochastic eco-evolutionary dynamics of the population, and can be simulated exactly (see Sec. 2 in SM [40]).

Importantly, here demographic fluctuations are *coupled* to the *colored non-Gaussian* environmental noise [39, 40] and encoded in the master equation (5). This contrasts with the discrete-time population dynamics of, for example Ref. [18], where external and internal noises are *independent and Gaussian*. Simulation results, see figure 1(c) and Ref. [62] (in which $N(0) = \langle K\rangle$, as in all our simulations), reveal that generally $N(t)$ evolves much faster than the population composition. We consider $K_+ > K_- \gg 1$ to ensure that, after a transient, $N(t)$ is at quasi-stationarity where it is characterized by its quasi-stationary distribution (N-QSD). The population eventually collapses after a time that diverges with the system size [51, 52], a phenomenon that can be disregarded for

our purposes. Below we study the eco-evolutionary dynamics in terms of the random variables N and x, focusing on the fixation properties of the population and its quasi-stationary distribution.

It is useful to start our analysis by considering the mean-field approximation which ignores *all noise* (say $K = \langle K\rangle$). In this case, the population size N and composition x evolve deterministically according to [26, 27, 39, 53]

$$\dot{N} = \sum_{\alpha=S,F} T_\alpha^+ - T_\alpha^- = N\left(g(x) - \frac{N}{K}\right), \qquad (6)$$

$$\dot{x} = \frac{T_S^+ - T_S^-}{N} - x\frac{\dot{N}}{N} = -sg(x)\frac{x(1-x)}{1-sx}, \qquad (7)$$

where the dot signifies the time derivative. Equation (7), reminiscent of a replicator equation [24], predicts that x relaxes on a timescale $t \sim 1/s \gg 1$ and eventually vanishes while, according to equation (6), $N(t)$ equilibrates to $N(t) = \mathcal{O}(K)$ in a time $t = \mathcal{O}(1)$.

III. PIECEWISE-DETERMINISTIC MARKOV PROCESS, MORAN MODEL & FIXATION PROBABILITIES

In this section, we review the effects of environmental and demographic noise separately, and compound them to obtain the fixation probabilities characterizing the population composition, as outlined in Ref. [39]. Here, these results provide the necessary background for the discussion in Sections IV and V of our main novel findings.

A. Environmental noise & Piecewise-deterministic Markov process

If the population is only subject to external noise (EN), it follows the *bivariate* piecewise-deterministic Markov process (PDMP) [58], defined by (7) and

$$\dot{N} = N\left\{g(x) - \frac{N}{\mathcal{K}} + \xi N\left(\frac{1}{\mathcal{K}} - \frac{1}{K_+}\right)\right\}, \qquad (8)$$

where $\mathcal{K} = 2K_+K_-/(K_+ + K_-)$ is the harmonic mean of K_+ and K_- [39]. Equation (8) is a stochastic differential equation with multiplicative DMN ξ of amplitude $N^2(K_+ - K_-)/(2K_+K_-)$ [40]; it reduces to the deterministic limit (6) when the EN is removed (i.e. $K_+ = K_-$).

Although the process is only subject to EN, the global growth rate $g(x)$ couples the evolutionary and ecological dynamics. To simplify the analysis, we introduce an effective parameter $q \geq 0$ (see Section III C 2) and assume a constant $g \equiv 1 + q$ [39], obtaining the single-variate effective process

$$\dot{N} = \mathcal{F}(N,\xi) = \begin{cases} \mathcal{F}_+(N) & \text{if } \xi = 1 \\ \mathcal{F}_-(N) & \text{if } \xi = -1, \end{cases} \qquad (9)$$

$$\text{with} \quad \mathcal{F}_\pm(N) \equiv N\left[1 + q - \frac{N}{K_\pm}\right], \qquad (10)$$

describing the evolution of a population of size $N(t)$ subject only to EN. According to (9) and (10), each environmental state ξ has a fixed point

$$N^*(\xi) = \begin{cases} N_+^* = (1+q)K_+ & \text{if } \xi = 1 \\ N_-^* = (1+q)K_- & \text{if } \xi = -1, \end{cases} \quad (11)$$

After $t = \mathcal{O}(1)$, the PDMP is at stationarity, characterized by a stationary probability density function (PDF) $p_{\nu,q}^*(N, \xi)$ (derived in the SM [40]). Central for our purposes are the features of the marginal stationary PDF $p_{\nu,q}^*(N) = p_{\nu,q}^*(N, \xi) + p_{\nu,q}^*(N, -\xi) \propto N^{-2}\left[(N_+^* - N)(N - N_-^*)N^{-2}\right]^{\frac{\nu}{1+q}-1}$ [53], giving the probability density of N regardless of the environmental state ξ (see Section 3 of [40] for a derivation). Depending on the sign of the exponent, the distribution may be unimodal or bimodal [39], but has always support $[N_-^*, N_+^*]$, on which $\mathcal{F}_+ \geq 0$ and $\mathcal{F}_- \leq 0$.

B. Internal noise & Fitness-dependent Moran process

Internal noise stems from the inherent stochasticity of individual birth and death events in the population; it ultimately causes fixation (one strain taking over the whole population), and hence determines the long-term population composition. When internal and ecological dynamics are coupled, which strain fixates has consequences on the population size, making the fixation phenomenon particularly important.

If internal noise is the only source of randomness (constant K), we can study its effects using the fitness-dependent Moran model [22, 23, 41, 59, 60], with constant size $N \equiv K$ [61]. To keep the population size constant, at each birth corresponds a death. Therefore, x increases by $1/N$ if an S individual is born and an F dies ($SF \to SS$ at rate $\widetilde{T}_S^+ = T_S^+ T_F^-/N$), and decreases by $1/N$ if an F individual is born, replacing a dead S ($SF \to FF$ at rate $\widetilde{T}_S^- = T_S^- T_F^+/N$), with

$$\widetilde{T}_S^+ = \frac{1-s}{1-sx}g(x)(1-x)xN, \quad \widetilde{T}_S^- = \frac{1}{1-sx}g(x)(1-x)xN.$$

The corresponding mean-field equation is again (7). For an initial fraction x_0 of S individuals, in the framework of the Fokker-Planck equation, the fixation probability of S is [22, 23, 41, 45] (see also Section 5.1 in SM [40])

$$\phi(x_0)|_N = \frac{e^{-Ns(1-x_0)} - e^{-Ns}}{1 - e^{-Ns}}. \quad (12)$$

The fixation probability of S thus becomes exponentially smaller the larger the population's (constant) size or selection intensity s are; and, notably, is independent of $g(x)$. In the following we assume $x_0 = 1/2$ and drop the initial condition for notational simplicity: $\phi|_N \equiv \phi(x_0)|_N$ and $\phi \equiv \phi(x_0)$. Clearly, the fixation probability of F is $\widetilde{\phi}|_N = 1 - \phi|_N$. In Section 5.1 of the SM [40], we also outline the main properties of the mean fixation times of the fitness-dependent Moran model. The most relevant for our purposes is the fact that, in both cases $b = 0$ and $b > 0$, the unconditional and conditional mean fixation times scale as $\mathcal{O}(1/s)$ to leading order when $s \ll 1$ and $Ns \gg 1$.

C. Fixation under switching carrying capacity

The strain S unavoidably goes extinct in the deterministic limit, see equation (7), and has an exponentially vanishing survival probability when K is constant, see equation (12). However, when the carrying capacity switches, the population undergoes "bottlenecks" that can enhance this probability [39] and alter the long-term average population size.

1. Fixation probabilities in the pure competition scenario ($b = 0$)

When $b = 0$, both species compete for the same finite resources, with a slight selective advantage to F. Therefore, N and x are solely coupled by demographic fluctuations. After a time $t = \mathcal{O}(1)$, N attains quasi-stationarity where it is distributed according to its N-QSD [62], that is well described by the PDF $p_{\nu/s}^* \equiv p_{\nu/s,0}^*(N)$. On the other hand, x relaxes on a much slower timescale $t \sim 1/s \gg 1$ and we showed that the mean fixation time scales as $\mathcal{O}(1/s)$ to leading order when $s \ll 1$ and $\langle K \rangle s \gg 1$ [39, 40, 53]. As a consequence, as shown in Section 5.2 of the SM [40], the population experiences, on average, $\mathcal{O}(\nu/s)$ environmental switches prior to fixation (see figures S6 in [40] and 1(c)). When $s \ll 1$ and $K_- \gg 1$, we can thus exploit this timescale separation and compute the S fixation probability ϕ by averaging $\phi|_N$ over $p_{\nu/s}^*$, with the rescaled switching rate $\nu \to \nu/s$ [39]:

$$\phi \simeq \int_{K_-}^{K_+} \phi|_N \, p_{\nu/s}^*(N) \, dN. \quad (13)$$

The PDF $p_{\nu/s}^*$ is sharply peaked at $N \simeq \mathcal{K}$ when $\nu \gg s$, whereas it has two sharp peaks at $N \simeq K_\pm$ when $\nu \ll s$. Equation (13) captures the limiting behavior $\phi \xrightarrow{\nu \to \infty} \phi|_\mathcal{K}$ when $\nu \gg s$ (many switches prior to fixation), resulting from the self-average of the EN (since $\xi(t) \xrightarrow{\nu \to \infty} \langle \xi(t) \rangle = 0$), as well as $\phi \xrightarrow{\nu \to 0} (\phi|_{K_-} + \phi|_{K_+})/2$ in the regime of rare switching ($\nu \ll s$), when the environment almost never changes prior to fixation [39]. As shown by figure S2 in Section 2 of the SM [40], equation (13) reproduces the simulation results for the fixation probability of S within a few percent over a broad range of ν values. While S remains less likely to fixate than F, its fixation probability is much higher than in a constant environment ($\phi \gg \phi|_{\langle K \rangle}$): environmental variability considerably offsets the evolutionary bias favoring F.

2. Fixation in the public good scenario, $b > 0$

In the public good scenario, $g(x) = 1 + bx$ with $0 < b = \mathcal{O}(1)$, S individuals act as public good producers (cooperators). The higher x, in fact, the higher the reproduction rate of

(a)

(b)
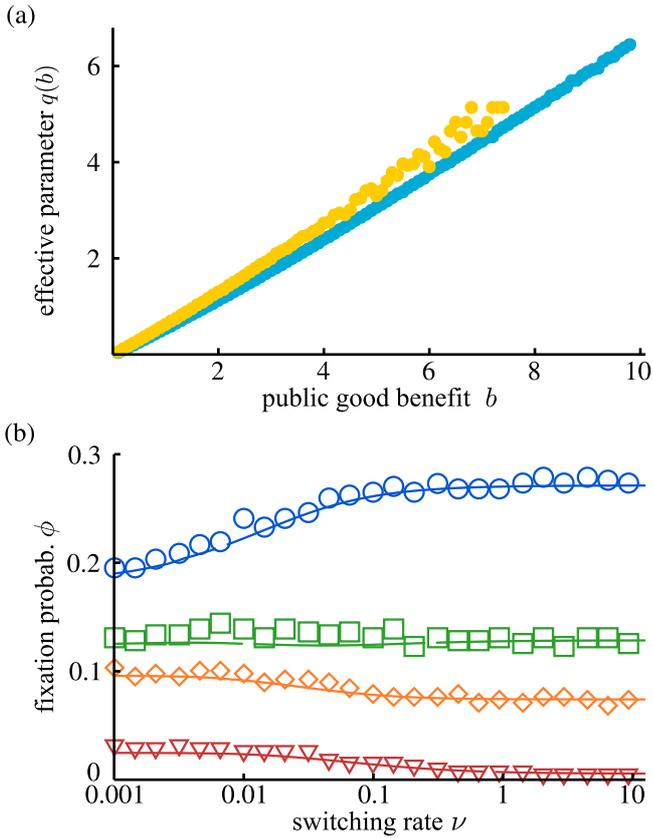
FIG. 2: (a) $q(b)$ vs. b for $s = 0.02$ (cyan) and $s = 0.05$ (yellow), see text. (b) ϕ vs. ν in the case $b > 0$: for $(s, b) = (0.02, 0.2)$ (blue, $\circ$), $(0.02, 2)$ (green, $\square$), $(0.05, 0.2)$ (orange, $\diamond$), $(0.05, 2)$ (red, ∇). Symbols are ϕ from simulations (10^4 runs) and solid lines show ϕ_q from the effective theory, see text. In all panels, other parameters are $(K_+, K_-, x_0) = (450, 50, 0.5)$.

both strains, see equations (2). However, since S bears alone the metabolic cost of cooperation (PG production), it grows slower than F and, deterministically, x decreases.

When $b > 0$, N and x are explicitly coupled, and they do not evolve on separate timescales: N is a fast variable, enslaved to the slow-varying x [62]. To determine the fixation probability, in Ref. [39] we devised an effective approach, based on suitably choosing the parameter q ($0 \leq q \leq b$) and setting $g(x) \equiv 1 + q$ in equation (8). This decouples N and x in an effective population whose size distribution, at quasi-stationarity and for any ν, is well described by the PDMP PDF $p_{\nu,q}^*(N)$. As outlined in Ref. [39], the fixation probability of S within this effective theory is determined similarly to the case $b = 0$ and is given by $\phi_q = \int_{N_-^*}^{N_+^*} \phi|_N \, p_{\nu/s,q}^*(N) \, dN$. As above, this expression simplifies in the limiting regimes of frequent/rare switching: $\phi_q \simeq \phi_q^{(\infty)} \equiv \phi|_{(1+q)\mathcal{K}}$ when $\nu \gg s$, and $\phi_q \simeq \phi_q^{(0)} \equiv (\phi|_{N_-^*} + \phi|_{N_+^*})/2$ when $\nu \ll s$. We determined the effective parameter $q = q(b)$ for given $(K_\pm, s, b)$ by matching the prediction of $\phi_q^{(\infty)}$ with the results of simulations (see [39] and SM [40]). Figure 2(a) shows that $q(b)$ increases almost linearly with b, and depends weakly on s.

Clearly, $q(0) = 0$ when $b = 0$, and ϕ_q thus reverts to (13).

Figure 2(b) shows that the effective approach captures the effects of the coupling between N and x for several choices of b and s, over a broad range of ν. As detailed in the SM [40], the predictions of ϕ_q agree within a few percent with simulation results when $s \ll 1$, while the accuracy deteriorates as s and b increase, therefore lowering ϕ. In fact, increasing b yields higher $q(b)$, which results in effectively increasing the carrying capacity $K_\pm \to (1 + q(b))K_\pm$. In the $\nu \to \infty, 0$ limits, this is equivalent to rescaling the selection intensity as $s \to (1 + q(b))s$, as inferred from $\phi_q^{(\infty,0)}$ and equation (12). Therefore ϕ decays (approximately) exponentially with b, as shown by figure 3(a).

IV. CORRELATIONS & COOPERATION IN THE ECO-EVOLUTIONARY GAME

After a time $t \gg 1/s$, fixation has very likely occurred and the population composition is fixed and consists of only F or S individuals. In this quasi-stationary regime, the population size $N(t)$ however keeps fluctuating, driven by the randomly switching carrying capacity $K(t)$. When the slow strain S produces a public good (PG), the long-time eco-evolutionary dynamics is characterized by the correlations between the population size and its composition. In this section, we analyze the long-term dynamics by computing the correlations first, and then by analyzing the ensuing "eco-evolutionary game".

To this end, it is useful to consider the average population size $\langle N \rangle_{\nu,b}^*$ for given ν and b, after a time $t \gg 1/s$, when the population is at *quasi-stationarity* and consists of only S or F individuals, see Section 5.2 in SM [40]. Within the PDMP approximation—that is, approximating the evolution of N by the PDMP (9), see Section 6.1 of SM [40]—we can compute the quasi-stationary average of N using the PDMP PDF $p_{\nu,q}^*$ (see also Sec. V A):

$$\langle N \rangle_{\nu,b}^* = (1 + b)\phi_b \langle N \rangle_{\frac{\nu}{1+b},0}^* + \widetilde{\phi}_b \langle N \rangle_{\nu,0}^* > \langle N \rangle_{\nu,0}^*, \quad (14)$$

where $\langle N \rangle_{\nu,0}^*$ is the population long-time average in the absence of PG production, ϕ_b denotes the fixation probability of S for a public good parameter b, and $\widetilde{\phi}_b = 1 - \phi_b$. Through equation (14), the PDMP approximation thus predicts that the long-term population size increases with b, see figure 3(b). Furthermore, while the fixation probabilities ϕ_b and $\widetilde{\phi}_b$ can increase or decrease with ν, the PDMP approximation predicts that the average population size at stationarity monotonically decreases with ν (see (S20)-(S22) in the SM [40]). Simulation results shown in figure 3(b) confirm that $\langle N \rangle_{\nu,b}^*$ increases with b, and decreases with ν (keeping other parameters constant).

A. Correlations between ecological & evolutionary dynamics

Equation (14) also highlights how fixation probabilities affect the long-term average population size. When $b > 0$, there
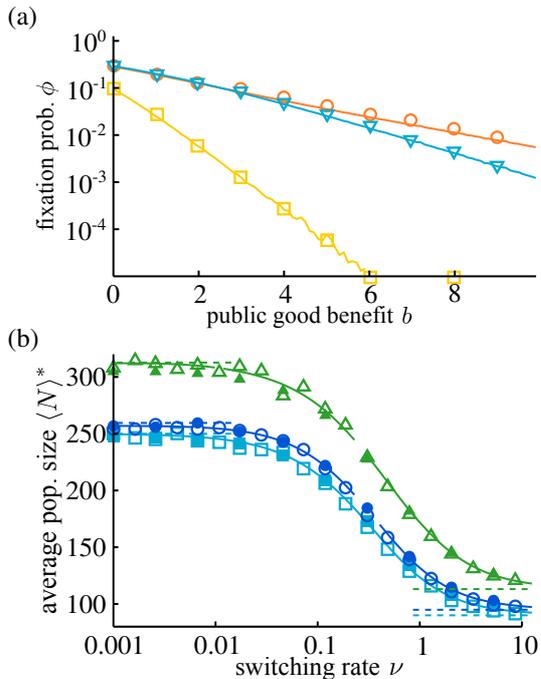
FIG. 3: (a) ϕ vs b in lin-log scale for $s = 0.02$, $\nu = 0.1$ (orange, $\circ$) and $\nu = 10$ (cyan, $\triangledown$); $s = 0.05$, $\nu = 10$ (yellow, $\square$). Lines are from ϕ_q, see text, and markers are from simulations. (b) $\langle N \rangle^*_{\nu,b}$ vs. ν for $b = 0$ (cyan, squares), $b = 0.2$ (blue, circles) and $b = 2$ (green, triangles) and $s = 0.02$. Solid lines are from (14); empty symbols are from simulations; filled symbols are from (25) within the linear noise approximation. Dashed lines indicate the predictions of (14) in the regimes $\nu \to \infty, 0$, see Section 6.1 in [40]. Parameters are $(K_+, K_-, x_0) = (450, 50, 0.5)$.

FIG. 4: (a) $\mathcal{C}^*_{\nu,b}$ vs b for $s = 0.05$ and $\nu \simeq 1$ (cyan, $\diamond$), $\nu = 0.1$ (yellow, $\triangledown$); $s = 0.02$ and $\nu = 1$ (red, $\square$), and $\nu = 0.1$ (orange, $\circ$). (b) $\mathcal{C}^*_{\nu,b}$ vs ν for $b = 2$ and $s = 0.05$ (red, $\triangledown$), $s = 0.02$ (green, $\triangle$); $b = 0.2$ and $s = 0.05$ (orange, $\diamond$), $s = 0.02$ (blue, $\circ$). In all panels, the parameters are $(K_+, K_-, x_0) = (450, 50, 0.5)$. Symbols are results from simulations and solid lines are from equation (16); dashed lines in panel (b) denote the analytical predictions of $\mathcal{C}_{\nu,b}$ in the limits $\nu \ll s$ and $\nu \gg 1$, see text.

are nontrivial correlations between population size and composition, and how $N(t)$ and $x(t)$ are correlated is of direct biological relevance, see *e.g.* [30, 31].

Prior to fixation, these correlations are accounted by the effective parameter $q(b)$ (see section III C 2). Here, we investigate their effect after fixation using the rescaled connected correlation function

$$\mathcal{C}_{\nu,b}(t) = \frac{\langle (N(t) - \langle N(t) \rangle)(x(t) - \langle x(t) \rangle) \rangle}{\langle N(t) \rangle \langle x(t) \rangle}, \quad (15)$$

where $\langle \cdot \rangle$ denotes the ensemble average. When $\langle N(t)x(t) \rangle = \langle N(t) \rangle \langle x(t) \rangle$, i.e. in absence of correlations, $\mathcal{C}_{\nu,b}(t)$ vanishes. At quasi-stationary, $t \gg 1/s$, we have $\langle N(t)x(t) \rangle \to \langle Nx \rangle^*_{\nu,b}$, $\langle N(t) \rangle \to \langle N \rangle^*_{\nu,b}$, $x \to 1$ or 0 with respective probability ϕ_b and $\widetilde{\phi}_b$, $\langle x(t) \rangle \to \phi_b$ and $\mathcal{C}_{\nu,b}(t) \to \mathcal{C}^*_{\nu,b}$. Within the PDMP approximation, using eq. (14) and $\phi_b \simeq \phi_q$, equation (15) becomes ($t \gg 1/s$)

$$\mathcal{C}^*_{\nu,b} = \frac{\langle Nx \rangle^*_{\nu,b}}{\langle N \rangle^*_{\nu,b} \phi_b} - 1 \simeq \frac{\widetilde{\phi}_q \left[(1+b)\langle N \rangle^*_{\frac{\nu}{1+b},0} - \langle N \rangle^*_{\nu,0} \right]}{(1+b)\phi_q \langle N \rangle^*_{\frac{\nu}{1+b},0} + \widetilde{\phi}_q \langle N \rangle^*_{\nu,0}}. \quad (16)$$

Since $\langle N \rangle^*_{\nu,0}$ is decreasing in ν (see figure 3(a)), this long-term correlation is always positive for $b \geq 0$, and vanishes only for $b = 0$.

As shown in figure 4, $\mathcal{C}^*_{\nu,b}$ grows approximately linearly with b and is non-monotonic in ν with a maximum for $\nu = \mathcal{O}(1)$; all features that equation (16) captures well. The ν-dependence of $\mathcal{C}^*_{\nu,b}$ stems from the fact that ϕ_b increases or decreases with ν, depending on the value of s, see figure 2(b) [39]. In the limiting regimes $\nu \to \infty, 0$, equation (16) simplifies and yields $\mathcal{C}^*_{\nu,b} \simeq b[1 - (1 + b)\phi^{(\infty,0)}_{q(b)}]$ [40]. Therefore, in these the limiting regimes $\mathcal{C}^*_{\nu,b}$ increases in s, and scales as $\mathcal{O}(b)$, as shown by figure 4, yielding $\langle Nx \rangle^* = (1 + \mathcal{O}(b))\langle N \rangle^*_{\nu,b} \phi^{(\infty,0)}_{q(b)}$.

These results show that, when species S provides a PG, there are nontrivial long-term correlations between *ecological and evolutionary variables*: the population size is shaped by its composition. The correlations between N and x are maximal in the intermediate switching regime where $\nu = \mathcal{O}(1)$ is comparable to the growth rate of N, and are weaker in the limiting switching regimes, on which we devised the effective theory of section III C 2.

B. When is cooperation beneficial? In which conditions is it best to cooperate?

Producing the public good (PG) slows the growth of the S strain, see equation (7) with $g(x) > 0$, and thus reduces exponentially the fixation probability of S, as shown in figure 3(a). On the other hand, the PG leads to higher average population sizes (see equation (14) and figure 3(b)) and therefore provides a long-term benefit to the whole population. At the population level, a "social dilemma" [24, 41] of sorts arises after fixation of either F or S: Cooperators pay a cost through their reduced fixation probability, while they provide a benefit, through the PG, by increasing the expected long-term number of individuals of both strains. We analyze the trade-off between benefit and cost of cooperation by introducing the notion of "eco-evolutionary game" in the context of a metapopulation of non-interacting communities: Each system realization (simulation run) corresponds to a community of time-fluctuating size, and the collection of the system's realizations constitutes the metapopulation [26, 27, 30, 31, 37], that is an ensemble of non-interacting communities. After fixation, each community consists of only S or F individuals. It is worth emphasizing that the social dilemma arising in the eco-evolutionary game differs from traditional games in a finite population of constant size [24, 41]: Although F is always more likely to fixate than S (when x_0 is not too close to 1, as in classical evolutionary games), communities consisting only of individuals of strain S can be of significantly larger size than those containing only F's thanks to their production of PG (allowing them to possibly attain the maximum carrying capacity $(1 + b)K_+$). In this eco-evolutionary game in a population of *time-varying size*, we thus propose to measure the evolutionary success of a strain in terms of the population size averaged after fixation over the ensemble of non-interacting communities, see also Section 6.2 of the SM [40]: The expected payoff of the game is hence the relative long-term average number of individuals of each strain, see below. Interestingly, this formulation of the eco-evolutionary game is of potential direct relevance to microbial experiments in which colonies of bacteria, some of which can produce a public good, are grown and compete in "a metapopulation of test tubes", see *e.g.* [30, 31, 36, 37].

Below, we use the PDMP approximation and simulations to investigate the relative abundance of each species at quasi-stationarity (see also Section 6.1 in [40]).

The average number of F individuals at quasi-stationarity, given a switching rate ν and PG parameter b is

$$\langle N_F \rangle^*_{\nu,b} = \langle N | x = 0 \rangle^*_{\nu,b} = (1 - \phi_b)\langle N \rangle^*_{\nu,0},$$

i.e. the average population size conditioned to F fixation. Similarly, the average number of cooperators S at quasi-stationarity is

$$\langle N_S \rangle^*_{\nu,b} = \langle N | x = 1 \rangle^*_{\nu,b} = (1 + b)\phi_b \langle N \rangle^*_{\nu/(1+b),0}.$$

In the context of the above eco-evolutionary game, we propose to measure the expected payoff provided by the PG as *the difference between the expected number of individuals of*

a strain at quasi-stationarity when $b > 0$ relative to the case $b = 0$. Hence, the expected payoff to F is

$$\Delta F_{\nu,b} \equiv \langle N_F \rangle^*_{\nu,b} - \langle N_F \rangle^*_{\nu,0} = (\phi_0 - \phi_b)\langle N \rangle^*_{\nu,0} > 0. \quad (17)$$

Since $\phi_0 > \phi_b$, see figure 3(b), this quantity is positive and increases with b. This means that, as in other social dilemmas, see, *e.g.*, Refs. [24, 41], the benefit of "freeriding" increases when the level of cooperation, here given by b, is raised. However, this does not rule out the possibility that, under certain circumstances, the PG production can be either beneficial or detrimental to S, and even permits S to be better off than F. In fact, the eco-evolutionary expected payoff for cooperators reads

$$\begin{aligned} \Delta S_{\nu,b} &\equiv \langle N_S \rangle^*_{\nu,b} - \langle N_S \rangle^*_{\nu,0} \\ &= (1 + b)\phi_b \langle N \rangle^*_{\frac{\nu}{1+b},0} - \phi_0 \langle N \rangle^*_{\nu,0}, \quad (18) \end{aligned}$$

and clearly varies nontrivially with ν and b. Unless $\Delta S_{\nu,b} > 0$, the PG is actually detrimental for cooperators: the expected number of S individuals is lower than it would be without PG. In this context, the PG benefits cooperators only if the increase in the average population size offsets the decrease in fixation probability, i.e. if

$$\Delta S_{\nu,b} > 0 \Leftrightarrow (1 + b)\frac{\langle N \rangle^*_{\frac{\nu}{1+b},0}}{\langle N \rangle^*_{\nu,0}} > \frac{\phi_0}{\phi_b}$$

In figure 5, we show that $\Delta S_{\nu,b}$ is non-monotonic in b, generating a maximum at an *optimal value* $b^*(\nu, s)$, which defines the conditions where PG production is the most rewarding for cooperators. Moreover, we observe a definite *critical threshold* $b_c(\nu, s)$, below which producing a PG benefits cooperators since $\Delta S_{\nu,b} > 0$.

Using our effective theory, $\phi \simeq \phi_{q(b)}$, and the PDMP approximation, the expected payoff of S (18) reads

$$\begin{aligned} \Delta S_{\nu,b} &= (1 + b)\phi_{q(b)} \int_{K_-}^{K_+} N p^*_{\frac{\nu}{1+b}}(N) \, dN \\ &\quad - \phi_0 \int_{K_-}^{K_+} N p^*_{\nu}(N) \, dN. \quad (19) \end{aligned}$$

When $\nu \to \infty$, the DMN self-averages ($\xi \to \langle \xi \rangle = 0$) and equation (18) is given by the expected payoff of S in a population of effective size $\langle N \rangle^*_{\infty,0} = \mathcal{K}$, see equation (S23) in the SM [40], yielding $\Delta S_{\infty,b} = [(1 + b)\phi_{q(b)}^{(\infty)} - \phi_0^{(\infty)}]\mathcal{K}$. Hence, when the DMN self-averages, the expected payoff of S is positive if $\phi_{q(b)}^{(\infty)} > \phi_0^{(\infty)}/(1 + b)$.

Results in figure 5 show that equation (19) approximates well the simulation results over a broad range of parameters. The root and the maximum of equation (19) provide (approximate) predictions for b_c and b^*, see figures 6 and S7(a) in the SM [40]. These figures reveal that b_c and b^* depend non-monotonically on ν and vary greatly with s, both behaviors well-captured by the theory. Figures 5 and S7(b) [40] also show that the maximal payoff for S can be significantly higher than that of F, especially when the selection s is low.
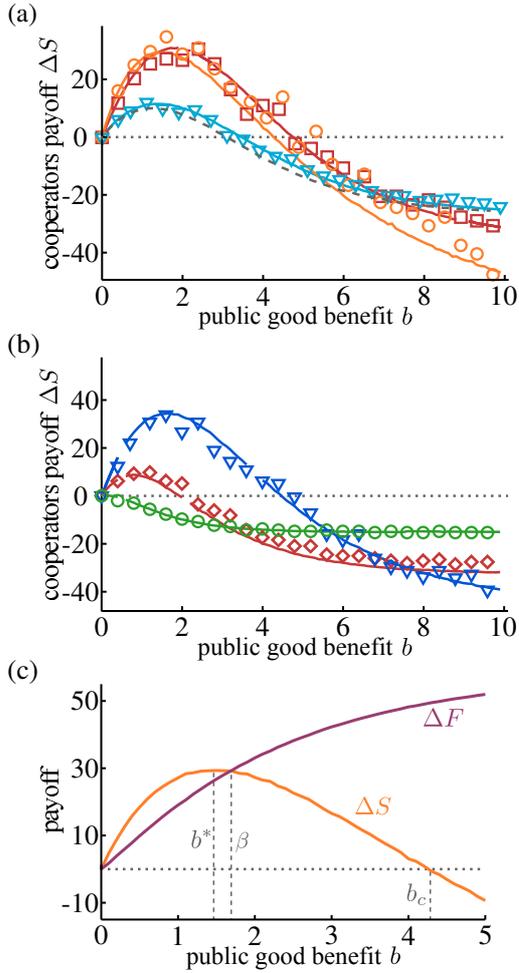
FIG. 5: (a) $\Delta S_{\nu,b}$ vs. b for $s = 0.02$ and switching rates $\nu = 10$ (cyan, ∇), $\nu = 1$ (red, $\square$), $\nu = 0.1$ (orange, $\circ$). Predictions from equation (19) (solid) are compared to simulation results (symbols). The grey dashed line corresponds to the predictions of $\Delta S_{\infty,b}$, see text. We find $\Delta S_{\nu,b} > 0$ when $0 < b < b_c(\nu,s)$ with an optimal payoff for S when $b = b^*(\nu,s)$, e.g. $(b_c, b^*) \approx (4.9, 2.1)$ at $\nu = 1$. (b) $\Delta S_{b,\nu}$ vs. b with $\nu \simeq 0.44$, for $s = 0.02$ (blue, ∇), $s = 0.03$ (red, $\diamond$), and $s = 0.05$ (green, $\circ$). Solid lines are from equation (19) and symbols are simulation results (see SM [40]). (c) Expected payoffs $\Delta S_{\nu,b}$ and $\Delta F_{\nu,b}$ vs. b for $s = 0.02$ obtained from equation (19). Dashed lines show the values of b^*, β and b_c. In all panels, the parameters are $(K_+, K_-, x_0) = (450, 50, 0.5)$.

FIG. 6: (a) b_c vs ν. Symbols are results from simulations and solid lines are from equation (19) for $s = 0.02$ (blue), $s = 0.03$ (orange), and $s = 0.05$ (green). (b) Heatmap of $(\Delta S_{\nu,b} - \Delta F_{\nu,b})/\langle N \rangle^*_{\nu,0}$, from equation (19) for $s = 0.02$. The gray dotted line shows $b = b_c(\nu,s)$, the dashed line $b = \beta(\nu,s)$ and the solid line $b = b^*(\nu,s)$. In the blue area (phases (i) and (ii)), $b > \beta$ and F is better off than S ($\Delta F_{\nu,b} > \Delta S_{\nu,b}$). PG production is detrimental for S in phase (i) where $b > b_c$ and $\Delta S_{\nu,b} < 0$; beneficial for S ($\Delta S_{\nu,b} > 0$) in phase (ii) where $\beta < b < b_c$, but more beneficial for F (higher expected payoff). In the red/pink area of region (iii), $b < \beta$ and S is better off than F ($\Delta S_{\nu,b} > \Delta F_{\nu,b}$), see text. Colored dots correspond to "gaps" in the numerical data (see [40]). Parameters are $(K_+, K_-, x_0) = (450, 50, 0.5)$.

In order to discuss the properties of the eco-evolutionary game, it is useful to determine the value $b = \beta(\nu,s)$ of equal expected payoff, i.e. such that which $\Delta S_{\nu,\beta} = \Delta F_{\nu,\beta}$, see figure 5(c). From equations (17)-(19), we find that $\beta(\nu,s)$ is the solution of

$$\frac{1}{1+\beta} \left(\frac{2\phi_0}{\phi_{q(\beta)}} - 1 \right) = \frac{\langle N \rangle^*_{\frac{\nu}{1+\beta},0}}{\langle N \rangle^*_{\nu,0}} = \frac{\int_{K_-}^{K_+} N p^*_{\frac{\nu}{1+\beta}} \, dN}{\int_{K_-}^{K_+} N p^*_\nu \, dN} . \quad (20)$$

So β is a nontrivial function of ν and s, see figure 6(b).

Given the parameters b and s of the eco-evolutionary game, we have studied the values of the switching rate ν for which

it is beneficial to cooperate by producing a public good, and determined three distinct phases represented in the diagram of figure 6(b):

(i) When $b > b_c$, the PG production is detrimental for S. The cost of cooperation outweighs its benefits and the expected payoff for S is negative ($\Delta S_{\nu,b} < 0$). The PG thus benefits only F.

(ii) When $\beta < b < b_c$, the PG production benefits S, but benefits F more ($0 < \Delta S_{\nu,b} < \Delta F_{\nu,b}$).

(iii) When $0 < b < \beta$, S reaps a higher expected payoff than F ($\Delta S_{\nu,b} > \Delta F_{\nu,b} > 0$). In this case, the benefit of the PG outweigh its cost, and its production is *favored*.

Within the above metapopulation interpretation of the eco-evolutionary game, species F effectively exploits S in phases (i) and (ii), but is at a disadvantage in phase (iii). Since the expected payoff to S is positive in regions (ii) and (iii), we say that *cooperation of a public good with benefit parameter b is beneficial when $0 < b < b_c(\nu, s)$, and advantageous for $0 < b < \beta(\nu, s)$*. Given a set of parameters (b, ν, s), PG production is the best strategy if two conditions are met: (a) the expected payoff of S is higher than that of F, which is satisfied in phase (iii); (b) b yields the maximum possible payoff for S, i.e., $b = b^*$. Hence, *in an environment switching at rate ν and under a selection intensity s, the best conditions to cooperate for the public good production is when the PG benefit parameter satisfies $b = b^*(\nu, s) < \beta(\nu, s)$*, represented by the solid gray line in phase (iii) of figure 6(b). It is also worth noting that this discussion also holds when the time-varying population size is not driven by the environmental noise: The limiting case $\nu \to \infty$, for which the DMN self-averages and the population reaches an effective size $N \to \mathcal{K}$, corresponds to the right end of the diagram of figure 6(b) where $\nu \gg 1$. Remarkably, environmental stochasticity yields several additional regimes in which cooperating becomes beneficial.

In the above context of a well-mixed population whose size fluctuates in time, this eco-evolutionary game shows that there are conditions under which PG production is beneficial for co-operators, and may even be the optimal strategy. This does not imply that the social dilemma, which still holds in its classical form prior to fixation, is resolved in general. However, this demonstrates that under environmental variability there are conditions in which cooperation (PG production), albeit disadvantaged in the short term, can be more successful than freeriding in the long term. In fact, although freeriders have a constant growth-rate advantage over cooperators and are always more likely to fixate (assuming $x_0 = 1/2$), here, the selective bias can be efficiently balanced by environmental variability, by allowing cooperators to be successful in forming, in the long term, larger communities than freeriders [40]. This can result in a greater increase of the long-term average number of cooperators than free-riders, and exemplifies the potential role of a fluctuating environment on the emergence of cooperative behavior in microbial communities.

V. LINEAR-NOISE AND PDMP APPROXIMATIONS TO THE POPULATION QSD

After $t \gg 1/s$, the population is likely to be at quasi-stationarity with its composition fixed [39]. Yet, the population size still fluctuates and $N(t)$ is distributed according to its quasi-stationary distribution. When $K_- \gg 1$, the population size is always large and, in the first instance, demographic fluctuations are negligible compared to environmental noise. In this case, eq. (9) characterizes reasonably well, albeit not fully, the long-term properties of $N(t)$.

A. Linear-noise approximation about the PDMP predictions

Throughout this work (and in [39]), we have shown that the PDMP approximation $p^*_{\text{PDMP},\nu,b}(N) = \phi p^*_{\nu,b}(N) + \widetilde{\phi} p^*_\nu(N)$ reproduces many characteristics of the quasi-stationary size distribution (N-QSD). However, as p^*_ν and $p^*_{\nu,b}$ only account for the external noise (EN), they cannot reproduce the complete N-QSD, which is also subject to internal noise (IN). Here, we use the linear noise approximation (LNA) about the PDMP predictions to account for the *joint effect* of the two noise sources, IN and EN, on the N-QSD.

The LNA is widely employed to quantify the effect of weak demographic fluctuations in the absence of external noise [45, 46], and has recently been used to study the joint effect of decoupled internal and external noise [12]. Here, we show how to generalize the LNA to the case where the population size fluctuates and demographic fluctuations are coupled to the external noise.

For our analysis, we assume that $K_+ \gtrsim K_- \gg 1$, so that $\langle K \rangle$ is large and of the same order as $K_\pm$ (see Section 7 in SM [40] for details). It is convenient to work with the continuous random variable $n = N/\Omega$, where $\Omega = \langle K \rangle \gg 1$ is the system's "large parameter". The auxiliary Markovian process $\{n(t), \xi(t)\}$ that we consider for the LNA is defined by $n \xrightarrow{\mathcal{T}^+} n + \Omega^{-1}$, $n \xrightarrow{\mathcal{T}^-} n - \Omega^{-1}$ and $\xi \xrightarrow{\nu} -\xi$, where the transition rates $\mathcal{T}^\pm$ are given by equations (S30) in the SM [40]. We also introduce $\psi = \lim_{\Omega \to \infty} N/\Omega = \mathcal{O}(1)$, which obeys the stochastic differential equation (S33) [40] defining the corresponding PDMP, and the random variable $\eta(t)$, capturing the fluctuations of n about ψ, according to

$$n(t) = \psi(t) + \frac{\eta(t)}{\sqrt{\Omega}}, \qquad (21)$$

We are interested in the (quasi-)stationary joint probability density $\pi^*_{\nu,q}(\eta, \psi, \xi)$ of the process $\{n(t), \xi(t)\}$. This probability density can be decomposed into $\pi^*_{\nu,q}(\eta, \psi, \xi) = \pi^*(\eta|\psi, \xi)\pi^*_{\nu,q}(\psi, \xi)$, where $\pi^*_{\nu,q}(\psi, \xi) = \Omega p^*_{\nu,q}(\Omega\psi, \xi)$ is the stationary joint PDF of the PDMP $\{\psi(t)\}$ and is readily obtained from the PDF of equation (9). The stationary probability density $\pi^*(\eta|\psi, \xi)$ accounts for the demographic fluctuations about $\{\psi(t)\}$ in the environmental state ξ. Following Ref. [12], we assume that the demographic fluctuations are approximately the same in both environmental states, i.e. $\pi^*_{\nu,q}(\eta|\psi, \xi) \simeq \pi^*_{\nu,q}(\eta|\psi, -\xi)$, and simply denote $\pi^*_{\nu,q}(\eta|\psi) \equiv \pi^*_{\nu,q}(\eta|\psi, \pm\xi)$. This assumption is reasonable when K_+ and K_- are of the same order, and yields

$$\pi^*_{\nu,q}(\eta, \psi, \xi) \simeq \pi^*(\eta|\psi)\pi^*_{\nu,q}(\psi, \xi). \qquad (22)$$

With this approximation, the quasi-stationary marginal LNA probability density of $\{n(t)\}$ is

$$\begin{aligned} \pi^*_{\nu,q}(n) &= \sum_{\xi=\pm 1} \int\int d\psi d\eta \, \pi^*(\eta|\psi) \\ &\times \pi^*_{\nu,q}(\psi, \xi) \, \delta\left(n - \psi - \frac{\eta}{\sqrt{\Omega}}\right), \end{aligned} \qquad (23)$$
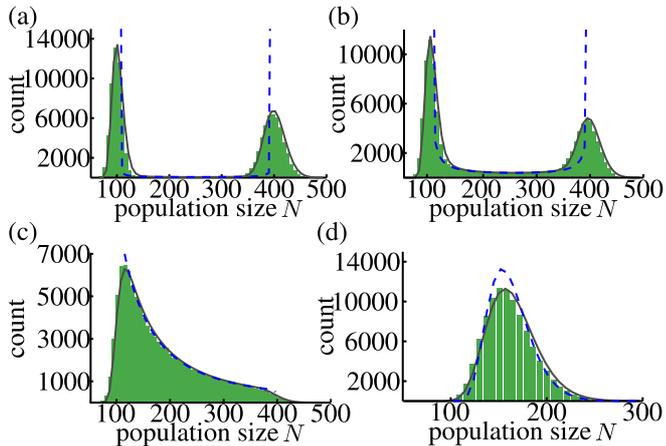
FIG. 7: Histograms of the population size distribution (N-QSD) when $b = 0$ (shaded area) compared with the predictions of the LNA (solid), from equation (S39) of the SM [40], and with the PDMP predictions (dashed), from $p^*_{\nu,0}$, for different switching rates: (a) $\nu = 0.01$, (b) $\nu = 0.1$, (c) $\nu = 1$, (d) $\nu = 10$, see text. Parameters are $(K_+, K_-, s, x_0) = (400, 100, 0.02, 0.5)$. Here, $\mathcal{K} = 160$.

where $\pi^*(\eta|\psi) = \exp\{-\eta^2/(2\psi)\}/\sqrt{2\pi\psi}$ (see SM [40] for details), and the Dirac delta ensures that (21) is satisfied. Calling $p^*_{\text{LNA},\nu,0}(N) = \pi^*_{\nu,0}(n)/\Omega$ and $p^*_{\text{LNA},\nu,b}(N) = \pi^*_{\nu,b}(n)/\Omega$, explicitly given by eqs. (S39) and (S40) in SM [40], the LNA quasi-stationary probability density reads

$$p^*_{\text{LNA},\nu,b}(N) = \phi p^*_{\text{LNA},\nu,b}(N) + \widetilde{\phi} p^*_{\text{LNA},\nu,0}(N). \quad (24)$$

Within the LNA, the quasi-stationary average population size is obtained by averaging N over $p^*_{\text{LNA},\nu,b}(N)$:

$$\langle N \rangle^*_{\text{LNA},\nu,b} = \int_0^\infty N p^*_{\text{LNA},\nu,b}(N)\, dN\,, \quad (25)$$

where, it is worth noting, the integral is no longer restricted to a finite support. As figure 3(b) shows, $\langle N \rangle^*_{\text{LNA},\nu,b}$ is as good an approximation of simulation results, as its PDMP counterpart $\langle N \rangle^*_{\nu,b}$ from equation (14). This is not surprising, and as done in Section IV, it is convenient to compute the averages of N using the PDMP approximation, i.e. by averaging over $p^*_{\text{PDMP},\nu,b}(N)$ as in eq. (14). However, as elaborated below, the LNA via the equation (24) gives an excellent characterization of the *full* N-QSD, well beyond the scope of the PDMP approximation.

B. LNA, N-QSD, and noise-induced transitions

1. Pure resource competition scenario, $b = 0$

In the pure resource competition scenario ($b = 0$), $p^*_{\text{LNA},\nu,0}(N) = \pi^*_0(n)/\Omega$ provides an excellent approximation of the N-QSD in all switching regimes, as shown in figure 7. In particular, $p^*_{\text{LNA},\nu,0}$ captures the noise-induced transition arising about $\nu = 1$ [39, 43, 44]: When $\nu < 1$, the switching
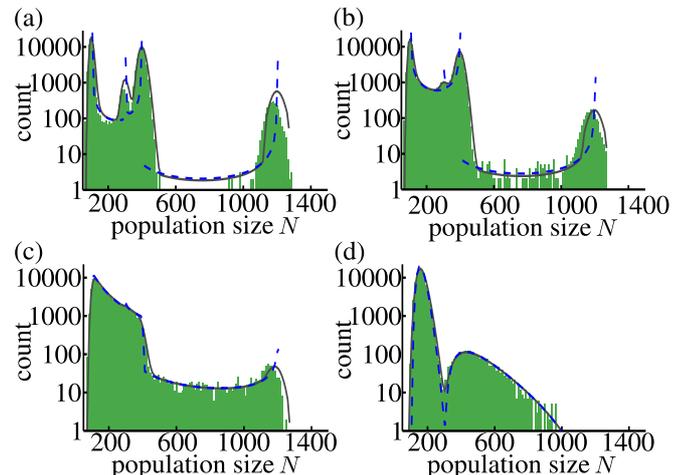
FIG. 8: Histograms of the population size distribution (N-QSD) when $b = 2$ (shaded area) compared with the predictions of the LNA (solid), from eq. (24) and equations (S39) and (S40) in the SM [40], and with the PDMP predictions (dashed) based on the PDF $p^*_{\nu,q}$, with $q = b$ (when $x = 1$) and $q = 0$ (when $x = 0$), for different switching rates: (a) $\nu = 0.01$, (b) $\nu = 0.1$, (c) $\nu = 1$, (d) $\nu = 10$. Parameters are $(K_+, K_-, s, b, x_0) = (400, 100, 0.02, 2, 0.5)$. For the analytical results, we have used the expression of ϕ_q for $\phi(b) \simeq \phi_{q(b)}$.

rate is lower than the population growth rate, and the N-QSD and $p^*_{\text{LNA},0}$ are both bimodal, with peaks at $N \approx K_\pm$, see figure 7 (a,b). When $\nu > 1$, the switching rate exceeds the population growth rate, and the N-QSD and $p^*_{\text{LNA},\nu,0}$ are thus unimodal, with a peak at $N \approx \mathcal{K}$, see Figure 7(c,d).

Figure 7 also shows that $p^*_{\text{LNA},\nu,0}(N)$ accurately predicts the peaks, their width and intensity, and the skewness of the N-QSD, whereas the PDMP predictions from $p^*_{\nu,q}(N)$ only captures the position of the peaks. This demonstrates how demographic fluctuations, aptly accounted for by the LNA, cause the discrepancies between the N-QSD and p^*_ν.

2. Public-good scenario, $b > 0$

The LNA expression (24) also provides an excellent approximation of the N-QSD in all switching regimes for the public good scenario ($b > 0$), see figure 8. In particular, $p^*_{\text{LNA},\nu,b}$ captures the noise-induced transitions arising about $\nu = 1$ and $\nu = 1 + b$ [39]: When $\nu < 1$, both conditional population distributions (for fixations to S or F) are bimodal, with different peaks. N-QSD and $p^*_{\text{LNA},\nu,b}$ thus have four peaks at $N \approx K_\pm$ and $N \approx (1 + b)K_\pm$, see figure 8(a,b). When $1 < \nu < 1 + b$, the S-conditional distribution is bimodal, whereas the F-conditional distribution is unimodal. The N-QSD and $p^*_{\text{LNA},\nu,b}$ thus have three peaks at $N \approx (1 + b)K_\pm$ and $N \approx \mathcal{K}$, see figure 8(c). Finally, when $\nu > 1 + b$, both conditional distributions are unimodal, but with different peaks. Hence, the N-QSD and $p^*_{\text{LNA},\nu,b}$ are bimodal with peaks at $N \approx \mathcal{K}$ and $N \approx (1 + b)\mathcal{K}$, see figure 8(d)

As figure 8 shows, $p^*_{\text{LNA},\nu,b}(N)$ provides a faithful charac-

terization of the N-QSD also when $b > 0$. This reiterates that the discrepancies with the PDMP approximation stem from demographic fluctuations. We also notice that the accuracy of the LNA slightly deteriorates near the lower-intensity peaks at high N and low ν (see figure 8(a)). These correspond to rare events, usually beyond the scope of the LNA. Moreover, in those regimes, some assumptions made in the derivation— *e.g.* equation (22)— reach the limit of their validity, see SM [40].

VI. CONCLUSION

We have studied the eco-evolutionary dynamics of a population subject to a randomly switching carrying capacity in which one strain has a slight selective advantage over another. In a model inspired by microbial communities evolving in fluctuating environments, we have considered two scenarios—one of pure resource competition (no interaction between strains) and one in which the slow (cooperating) strain produces a public good—and investigated the *coupled* effect of demographic and environmental noise.

The population composition has been characterized by the fixation probabilities, computed using the analytical procedure devised in Ref. [39], and, when a public good is produced, shown to be non-trivially correlated with the evolution of the population size. As a result, the production of public good gives rise to an *eco-evolutionary game*: On the one hand, producing the public good lowers the survival/fixation probability of cooperators; on the other hand, it also increases their population size. A social dilemma of sorts therefore ensues and, in a fluctuating environment, it is a priori not intuitively clear whether there are circumstances under which it is beneficial to produce a public good and what these conditions may be. Since we consider the eco-evolutionary game in a population of fixed composition (after fixation) but whose size fluctuates, we have proposed to measure the evolutionary benefit of the public good in terms of the long-term expected number of individuals of each strain. This is done in the biologically-inspired setting of a metapopulation of non-interacting communities of varying size composed uniquely by one of the species. In certain circumstances, that we have determined, the public good production allows the communities composed of cooperating S individuals to achieve a greater long-term increase of their average size than the communities consisting of freeriding F individuals. In these conditions, we say that the cooperating strain outcompetes the freeriding one. We have thus determined, both analytically and with simulations, the circumstances under which cooperation is beneficial or detrimental to public good producers, as well as the conditions under which it is the optimal strategy. Hence, we have demonstrated that the rate of switching, along with the selection in-

tensity and the public good parameter, determine when one species is more successful than another. Our analysis of the "eco-evolutionary game" thus shows that in a fluctuating population the evolutionary success of a strain goes beyond having a growth-rate advantage and a higher fixation probability.

We have also advanced the characterization of the population size distribution by generalizing the linear noise approximation to populations of fluctuating size, thus accounting for demographic fluctuations about the predictions of the underlying piecewise deterministic Markov process. While we have found that the linear noise and the piecewise-deterministic Markov process approximations describe the average population size equally well, only the former fully characterizes the population size distribution. In fact, the linear noise approach accounts for the joint effect of environmental and demographic noise and has allowed us to capture the width and skewness of the population size distribution.

This study shows that coupled environmental and demographic noise can greatly influence how the composition and size of a population evolve. In particular, social interactions between strains—such as public good production—can lead to intricate eco-evolutionary dynamics, which potentially support cooperation. This sheds light on phenomena that are directly relevant to microbial communities, which often feature coupled internal and ecological evolution. This can yield the kind of eco-evolutionary game analyzed here, that can be a potential theoretical framework for experimental studies investigating the emergence of cooperative behavior in microbial communities of time-fluctuating size.

[1] Morley C R, Trofymow J A, Coleman D C, Cambardella C. 1983 Effects of freeze-thaw stress on bacterial populations in soil microcosms. *Microbiol. Ecol.* **9**, 329-340. (doi: 10.1007/BF02019022)

[2] Fux C A, Costerton J W, Stewart P S, Stoodley P. 2005 Survival strategies of infectious biofilms. *Trends Microbiol.* **13**, 34-40. (doi: 10.1016/j.tim.2004.11.010)

[3] May R M.1973 *Stability and complexity in model ecosystems*. Princeton, USA: Princeton University Press.

[4] Karlin S, Levikson B. 1974 Temporal fluctuations in selection intensities: Case of small population size *T. Pop. Biol.* **74**, 383-412. (doi: 10.1016/0040-5809(74)90017-3)

[5] Kussell E, Leibler S. 2005 Phenotypic Diversity, Population Growth, and Information in Fluctuating Environments *Science* **309**, 2075-2078. (doi: 10.1126/science.1114383)

[6] Assaf M, Roberts E, Luthey-Schulten Z, Goldenfeld N. 2013 Extrinsic Noise Driven Phenotype Switching in a Self-Regulating Gene. *Phys. Rev. Lett.* **111**, 058102 (2013). (doi: 10.1103/PhysRevLett.111.058102)

[7] He Q, Mobilia M, Täuber U C. 2010 Spatial rock-paper-scissors models with inhomogeneous reaction rates. *Phys. Rev. E* **82**, 051909. (doi: 10.1103/PhysRevE.82.051909)

[8] Dobramysl U, Täuber U C. 2013 Environmental Versus Demographic Variability in Two-Species Predator-Prey Models. *Phys. Rev. Lett.* **110**, 048105. (doi: 10.1103/PhysRevLett.110.048105)

[9] Assaf M, Mobilia M, Roberts E. 2013 Cooperation Dilemma in Finite Populations under Fluctuating Environments. *Phys. Rev. Lett.* **111**, 238101. (doi: 10.1103/PhysRevLett.111.238101)

[10] Ashcroft P, Altrock P M, Galla T. 2014 Fixation in finite populations evolving in fluctuating environments. *J. R. Soc. Interface* **11**, 20140663. (doi: 10.1098/rsif.2014.0663)

[11] Melbinger A, Vergassola M. 2015 The Impact of Environmental Fluctuations on Evolutionary Fitness Functions *Scientific Reports* **5**, 15211. (doi: 10.1038/srep15211)

[12] Hufton P G, Lin Y T, Galla T, McKane A J. 2016 Intrinsic noise in systems with switching environments. *Phys. Rev. E* **93**, 052119. (doi: 10.1103/PhysRevE.93.052119)

[13] Hidalgo J, Suweis S, Maritan A. 2017 Species coexistence in a neutral dynamics with environmental noise. *J. Theor. Biol.* **413**, 1-10. (doi: 10.1016/j.jtbi.2016.11.002)

[14] Danino M, Shnerb N M. 2018 Fixation and absorption in a fluctuating environment. *J. Theor. Biol.* **441**, 84-92. (doi: 10.1016/j.jtbi.2018.01.004)

[15] Chesson P L, Warner R R. 1981 Environmental Variability Promotes Coexistence in Lottery Competitive Systems. *American Naturalist* **117**, 923-943. (doi: 10.1086/283778)

[16] Kussell E, Kishony R, Balaban N Q, Leibler S. 2005 Bacterial Persistence: A Model of Survival in Changing Environments. *Genetics* **169**, 1807-1814. (doi: 10.1534/genetics.104.035352)

[17] Acer M, Mettetal J, van Oudenaarden A. 2008 Stochastic switching as a survival strategy in fluctuating environments. *Nature Genetics* **40**, 471-475. (doi: 10.1038/ng.110)

[18] Loreau, M, de Mazancourt C. 2008 Species synchrony and its drivers: neutral and noneutral community dynamics in fluctuating environments *American Naturalist* **172**, E49-E66. (doi:10.1086/589746)

[19] Beaumont H, Gallie J, Kost C, Ferguson G, Rainey P. 2009 Experimental evolution of bet hedging Nature **462**, 90-93. (doi: 10.1038/nature08504)

[20] Visco P, Allen R J, Majumdar S N, Evans M R. 2010 Switching and Growth for Microbial Populations in Catastrophic Responsive Environments. *Biophys. J.* **98**, 1099-1108. (doi: 10.1016/j.bpj.2009.11.049)

[21] Xue B, Leibler S. 2017 Bet-hedging against demographic fluctuations *Phys. Rev. Lett.* **119**, 108113. (doi: 10.1103/PhysRevLett.111.058102)

[22] Crow J F, Kimura M, 2009 *An Introduction to Population Genetics Theory*. New Jersey, USA: Blackburn Press

[23] Blythe R A, McKane A J. 2007 Stochastic models of evolution in genetics, ecology and linguistics *J. Stat. Mech.* **P07018** (doi:10.1088/17442-5468/2007/07/P07018)

[24] Nowak M A, 2006 *Evolutionary Dynamics*. Cambridge, USA: Belknap Press

[25] Roughgarden J 1979 *Theory of Population Genetics and Evolutionary Ecology: An Introduction*. New York, USA: Macmillan.

[26] Melbinger A, Cremer J, Frey E. 2010 Evolutionary Game Theory in Growing Populations. *Phys. Rev. Lett.* **105**, 178101. (doi:10.1103/PhysRevLett.105.178101)

[27] Cremer J, Melbinger A, Frey E. 2011 Evolutionary and population dynamics: A coupled approach. *Phys. Rev. E* **84**, 051921. (doi: 10.1103/PhysRevE.84.051921)

[28] Pelletier F, Garant D, Hendry H P. 2009 Eco-evolutionary dynamics. *Phil. Trans. R. Soc. B* **364** 1483-1489. (doi:10.1098/rstb.2009.0027)

[29] Harrington K I, Sanchez A. 2014 Eco-evolutionary dynamics of complex strategies in microbial communities. *Communicative & Integrative Biology* **7:1**, e28230:1-7. (doi:10.4161/cib.28230)

[30] Chuang J S, Rivoire O, Leibler S. 2009 Simpson's Paradox in a Synthetic Microbial System. *Science* **323**, 272-275. (doi: 10.1126/science.1166739)

[31] Melbinger A, Cremer J, Frey E. 2015 The emergence of cooperation from a single mutant during microbial life cycles. J. R. Soc. Interface **12**, 20150171. (doi: 10.1098/rsif.2015.0171)

[32] Wahl L M, Gerrish P J, Saika-Voivod I. 2002 Evaluating the impact of population bottlenecks in experimental evolution. *Genetics* **162**, 961-971. (url: http://www.genetics.org/content/162/2/961)

[33] Patwas Z, Wahl L M. 2009 Adaptation rates of lytic viruses depend critically on whether host cells survive the bottleneck. *Evolution* **64**, 1166-1172. (doi: 10.1111/j.1558-5646.2009.00887.x)

[34] Brockhurst M A, Buckling A, Gardner A. 2007 Cooperation Peaks at Intermediate Disturbance. *Curr. Biol.* **17**, 761-765. (doi: 10.1016/j.cub.2007.02.057)

[35] Brockhurst M A. 2007 Population Bottlenecks Promote Cooperation in Bacterial Biofilms. PLoS One **7**, e634. (doi: 10.1371/journal.pone.0000634)

[36] Wienand K, Lechner M, Becker F, Jung H, Frey E. 2015 Non-Selective Evolution of Growing Populations. PloS one, **10(8)**, e0134300. (doi: 10.1371/journal.pone.0134300)

[37] Becker F, Wienand K, Lechner M, Frey E, Jung H. 2018 Interactions mediated by a public good transiently increase cooperativity in growing Pseudomonas putida metapopulations. Scientific Reports, **8**, 4093. (doi: 10.1038/s41598-018-22306-9)

[38] Rainey P B, Rainey K. 2003 Evolution of cooperation and conflict in experimental bacterial populations *Nature* **425**, 72. (doi: 10.1038/nature01906)

[39] Wienand K, Frey E, Mobilia M. 2017 Evolution of a Fluctuating Population in a Randomly Switching Environment. *Phys. Rev. Lett.* **119**, 158301. (doi:10.1103/PhysRevLett.119.158301)

[40] Wienand K, Frey E, Mobilia M. 2018 *Supplementary Material. fighshare https://doi.org/10.6084/m9.figshare.5683762.* (doi:10.6084/m9.figshare.5683762)

[41] Cremer J, Reichenbach T, Frey E. 2009 The edge of neutral evolution in social dilemmas *New J. Phys.* **11**, 093029. (doi: 10.1088/1367-2630/11/9/093029)

[42] Here, in reference to microbial communities, we use interchangeably use the terms "species" and "strain".

[43] Horsthemke W, Lefever R. 2006 *Noise-Induced Transitions*. Berlin, Germany: Springer

[44] Bena I. 2006 Dichotomous Markov noise: Exact results for out-of-equilibrium systems. A review. *Int. J. Mod. Phys. B* **20**, 2825-2889. (doi: 10.1142/S0217979206034881)

[45] Gardiner C W. 2002 *Handbook of Stochastic Methods* New York, USA: Springer

[46] van Kampen N G. 2003 *Stochastic Processes in Physics and Chemistry* Amsterdam, The Netherlands: North-Holland Publishing

[47] Kitahara K, Horsthemke W, Lefever R. 1979 Coloured-noise-induced transitions: exact results for external dichotomous Markovian noise. *Phys. Lett.* **70A**, 377-380. (doi: 10.1016/0375-9601(79)90336-0)

[48] Hänggi P, Talkner P. 1981 Non-Markov processes: The problem of the mean first passage time. *Z. Phys. B* **45**, 79-83. (doi: 10.1007/BF01294279)

[49] Van den Broek C, Hänggi P. 1984 Activation rates for nonlinear stochastic flows driven by non-Gaussian noise. *Phys. Rev. A* **30**, 2730-2736. (doi: 10.1103/PhysRevA.30.2730)

[50] Sancho J M. 1985 External dichotomous noise: The problem of the mean-first-passage time. *Phys. Rev. A* **31**, 3523(R)-3526(R). (doi: 10.1103/PhysRevA.31.3523)

[51] Spalding C, Doering C R, Flierl G R. 2017 Resonant activation of population extinctions. *Phys. Rev. E* **96**, 042411. (doi: 10.1103/PhysRevE.96.042411)

[52] A finite population unavoidably collapses into $(N, x) = (0, 0)$ where it is extinct [51]. This phenomenon is practically unobservable when $K_- \gg 1$ and occurs after lingering in the system's quasi-stationary state (where N is distributed according to its N-QSD) and much after the fixation of one species.

[53] Wienand K, Frey E, Mobilia M. 2017 *http://link.aps.org/supplemental/10.1103/PhysRevLett.119.158301*. (doi: 10.1103/PhysRevLett.119.158301)

[54] Cremer J, Arnoldini M, Hwa T. 2017 Effect of water flow and chemical environment on microbiota growth and composition in the human colon. *Proc. Nat. Acad. Sci.* **25**, 6438-6443. (doi: 10.1073/pnas.1619598114)

[55] Lindsey H A, Gallie J, Taylor S, Kerr B. 2013 Evolutionary rescue from extinction is contingent on a lower rate of environmental change. *Nature* **494**, 463-467. (doi: 10.1038/nature11879)

[56] Lambert G, Kussell E. 2015 Quantifying Selective Pressures Driving Bacterial Evolution Using Lineage Analysis. *Phys. Rev. X* **5**, 011016. (doi: 10.1103/PhysRevX.5.011016)

[57] Lechner M, Schwarz M, Opitz M, Frey E. 2016 Hierarchical Post-transcriptional Regulation of Colicin E2 Expression in *Escherichia coli*. *PLOS Comp. Biol.* **12**, e1005243. (doi: 10.1371/journal.pcbi.1005243)

[58] Davis M H A. 1984 Piecewise–deterministic Markov processes: a general class of nondiffusion stochastic models *J. R. Stat. Soc. B* **46**, 353-388. (Retrieved from http://www.jstor.org/stable/2345677)

[59] Moran P A P. 1962 *The statistical processes of evolutionary theory*. Oxford, UK: Clarendon

[60] Antal I, Scheuring I. 2006 Fixation of Strategies for an Evolutionary Game in Finite Populations *Bull. Math. Biol.* **68**, 1923-1944. (doi: 10.1007/s11538-006-9061-4)

[61] Otto S P, Whitlock M C. 1997 The Probability of Fixation in Populations of Changing Size. *Genetics* **146**, 723-733. (url: http://www.genetics.org/content/146/2/723)

[62] Wienand K, Frey E, Mobilia M. 2017 *fighshare https://doi.org/10.6084/m9.figshare.5082712*. (doi:10.6084/m9.figshare.5082712.v5)